PORT SAID ENGINEERING RESEARCH JOURNAL

Faculty of Engineering - Port Said University
Volume 27 No. 4 pp: 1:15

Numerical Assessment of RC Building Deformations Resting on Soil Containing Voids with Various Sizes and Locations

*Aya G. Abdel-Nasser [1 *], Emad Y. Abdel-Galil [2] and Ezzaat A. Sallam[3]*

[1]*Civil Engineering Department, Faculty of Engineering, Port Said University, Email: aya.gamal@eng.psu.edu.eg*
[2]*Civil Engineering Department, Faculty of Engineering, Port Said University, Email: emad0057@eng.psu.edu.eg*
[3]*Civil Engineering Department, Faculty of Engineering, Port Said University, Email: Ezzat.sallam@eng.psu.edu.eg*
[*]*Corresponding author, DOI: 10.21608/PSERJ.2023.226664.1254*

Received 3-8-2023
Revised 30-8-2023
Accepted 11-9-2023

ABSTRACT

Construction of reinforced concrete buildings on soils with unknown underground void locations may lead to building instability and tilting. The current study investigates the influence of the existence of underground voids on surface-reinforced concrete structures under gravity loads only. A numerical analysis using a finite element program (ANSYS) was performed to study the behavior of reinforced concrete buildings with different widths and heights. The buildings were rested on clay soil with a continuous circular void for a wide variety of void diameters and locations from the building's footing. Charts for settlements and differential settlements between footing edges for all cases were obtained to evaluate the effect of these parameters on the behavior of surface buildings. Based on the obtained results, equations for design were provided for the critical area underneath concrete structures affected by underground voids, according to the building size, void location, and diameter. These equations introduce simple tools to predict the critical void location within the variety of parameters that have been studied in this study.

Keywords: Underground void, Critical locations, Footing width, Void depth, Void eccentricity, Void diameter.

1 INTRODUCTION

The existence of underground voids beneath RC structures requires special attention because underground voids can influence the stability and tilting of those structures. That voids occur for various reasons, such as the dynamic loads occur by mining and tunneling works, ice melting below the surface, the melting of soluble materials such as gypsum, salt, dolomite, and limestone, and the disintegration of methane hydrate [1]. Also, it may be formed due to old tubes and the settlement of the backfill of the trench, which is poorly compacted. When the void is located below the foundation of the structures, remarkable bearing capacity and settlement troubles may occur, which cause costly and dangerous effects [2].

Several studies were conducted to estimate the stability of footings founded on soil with different cases of void shapes and locations. Using a finite element method, Baus [3] investigated the performance of strip footings centered on the continuous void in homogeneous soil. Baus and Wang [4] also studied experimentally and analytically the bearing capacity behavior of a strip footing placed on a continuous void in a silty clay soil type. Furthermore, Badie [5] and Badie and Wang [6] performed theoretical and experimental studies on the stability of foundations resting on compacted clay soil containing voids at different locations. In addition, Wang and Badie [7] investigated the effect of the existence of underground voids on the stability of shallow footing supported by compacted clay soil using a 3D finite element program. Also, Wang and Hsieh [8] used the upper bound theory of limit analysis to determine the collapse load of footings resting above continuous circular voids. Wang and Hsieh [8] and Jaroudi [9] developed equations that relate the footing collapse pressure to the size and location of the void. Badie and Wang [10] studied the effect of different

shapes of voids on footing behavior, two parallel strip footings above a single void below and one strip footing above two cavities. Lee *et al.* also investigated the vertical bearing capacity of strip footings above clay soil with single and dual continuous voids [1]. Hsieh and Wang [11] performed a group of analyses using a FE computer program for surface strip foundations subjected to central vertical loading rested on a continuous circular void. Kiyosumi *et al.* [12] used 2D plane strain finite-element analysis to study the effect of multiple voids on the yielding pressure of strip foundations. Kiyosumi *et al.* [13] conducted a set of loading tests on stiff soil containing square continuous voids. Lee and Kim [14] determined the collapse loads of strip rigid foundations placed on sand soil with single and dual continuous voids. Design charts were conducted to estimate the bearing capacity according to the dimensionless parameters, such as the void location from the footing, the void's shape, spacing between voids, and the soil friction angle. Lavasan *et al.* [15] examined numerically the bearing capacity and mechanism of failure for a shallow strip footing resting above twin voids. Zhao *et al.* [16] used the FE method to examine the stability analysis of irregular underground cavities.

Several studies also examined the effect of underground voids on foundations. Hsieh [17] used a finite element program to study the performance of strip footings underlain by continuous circular voids with three different soil types. Azam *et al.* [18] developed a finite-element analysis to investigate the behavior of strip foundations on a layered deposit of two soil layers and a uniform soil surface, both without and with a continuous void. Das and Khing [19] experimentally estimated the ultimate bearing capacity variation of a strip footing rested on sand soil underlain by a clay soil layer, with and without geogrid reinforcement, that is located at the interface between the two soil types. The effects of the presence of rectangular voids in clay soil were also studied. Sireesh *et al.* [20] conducted a set of laboratory tests to study the potential benefits of supply of geocell reinforced sand beds over clay subgrade with void including. Moghaddas Tafreshi *et al.* [21] presented results from strip foundations tested using a lab model resting on reinforced sand beds above a continuous void to investigate the advantages of replacing reinforced sand layers for bridging the underground void. Hussein [22] also conducted a series of numerical analyses for strip foundations resting on sand beds with continuous circular voids. Hussein developed an equation that provides good data for designing continuous footing, which centered on an underground void. Jayamohan *et al.* [23] conducted a series of laboratory tests to examine how an underground void affects the load settlement behavior of a strip foundation. They also studied the beneficial effects of the addition of a foundation bed and reinforced foundation bed on the load settlement behavior of the soil with voids. Anaswara and Shivashankar [24] numerically studied the behavior of one and two adjacently placed strip footings above granular beds underlain by weaker soil with and without voids. Mazouz *et al.* [25] examined the effects of the presence of an underground void on the bearing capacity of a strip foundation above an unreinforced and reinforced sand slope with geogrid with a void by using 2D plane-strain FEM analysis (PLAXIS). Xiao *et al.* [26] used finite element limit analysis (OptumG2) to study the undrained stability of strip footings underlain by voids in two clay layers. Zhou *et al.* [27] studied the bearing capacity and failure mechanism of footings rested on cohesive and frictional (c–φ) soils that contain voids.

Studying the effects of eccentric loading on footing rested above voids were also examined. Wang *et al.* [28] developed the finite element analysis to investigate the effect of voids on footing performance under eccentric and inclined loading. Lee *et al.* [29] analyzed the influence of load inclination on the bearing capacity of surface spread footings on undrained homogeneous clay soil with one and dual continuous voids using FE analysis. Mansouri *et al.* [30] performed an experimental study to examine the effect of underground circular voids on a strip foundation resting on the end of a cohesionless slope and loaded with eccentric loads. Gaoqiao Wu [31] studied the effect of eccentric loads on the footing bearing capacity founded on single and dual continuous voids.

Previous studies mainly focused on the behavior of footings rested on soil with voids without considering the soil-structure interaction and the nonlinearity behavior of the concrete structure. There is a severe dearth of studies investigating 3D fully reinforced concrete structures resting on soil with voids. Also, the influence of the different sizes of real 3D reinforced concrete buildings (areas and heights) due to voids' existence needs more research. The current study focused on the stability of the reinforced concrete structures resting on clay soil with voids using the finite element method with different areas and heights considering the soil-structure interaction.

2 MATERIALS AND METHODS

ANSYS, the finite element computer program, was used to simulate 3D reinforced concrete buildings resting on clay soil with and without void beneath them. The symmetric half part of the model was analyzed with the symmetry region option to reduce the number of elements in the analyses. In the current analysis, the effects of underground voids were investigated under the gravity loads of the structures. Loads of floor slabs and walls were applied as distributed loads on the adjacent beams in the floor. Material and structural modeling used in this numerical analysis is presented in the following section.

2.1 Material Modeling

2.1.1 Soil Model

The soil response was modeled as an isotropic, linearly elastic-perfectly plastic material using the Mohr-Columb model in ANSYS. Clay soil used in this analysis has a uniform unit weight (γ_{soil} =17.2 kN/m^3) with Young's modulus E_{soil}=40 Mpa, Poisson's ratio v= 0.4, and friction and dilation angles were set to be zero $\phi = \psi = 0$ to simulate the clay soil case.

2.1.2 Concrete Model

The nonlinear concrete material model for concrete structure members and footings assumed ascending and descending branches of the concrete stress-strain curve as a second-order parabola curve and a linear inclined line, respectively, and a linear model for tensile strains was considered. Where, concrete Young's modulus E_c=30,000 Mpa, Poisson ratio v = 0.2, and a uniform unit weight γ_c =22.5 kN/m^3.

2.1.3 Reinforcing Steel Model

An elastic-perfectly plastic model with a small inclined line was considered for the reinforcement in beams and columns. Where, steel Young's modulus E_s=200,000 Mpa and Poisson ratio v = 0.3.

2.2 Structural Modeling

2.2.1 Soil

The soil was modeled as a solid element (SOLID 185) in ANSYS. The horizontal and vertical boundaries of the soil model were chosen far enough away to have no impact on the results obtained. After a series of trial analyses, the external boundaries were positioned five and ten times the footing width (5*B* and 10*B*) horizontally from the foundation edge and vertically under the ground level, respectively. The vertical boundaries were modeled to be free in the vertical direction only, but the bottom side of the soil block was modeled to be fixed in all directions. The number of soil elements was increased in the area adjacent to the footing and the void location. Figure 1 shows the mesh elements and the boundaries of the soil block for half part of the symmetric model.

2.2.2 Reinforced Concrete Structure

Footings, columns, and beams were modeled as solid nonlinear concrete elements (SOLID 185) with reinforcement modeled as a beam element embedded on those concrete elements using (reinforcement model type) in ANSYS workbench, as shown in Figure 2.

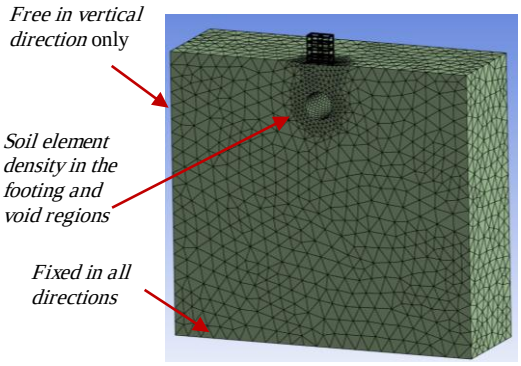

Figure 1: Mesh elements and soil block boundaries for the half part of the symmetric model

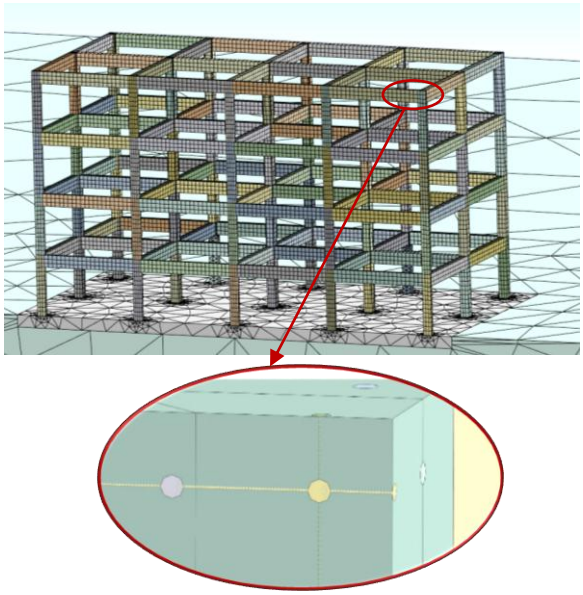

Figure 2: Reinforced concrete structure model

2.3 Verification of Numerical Model

To verify the efficiency of the numerical model developed for this study, the most relevant case study from the literature has been numerically modeled using ANSYS, and the results obtained were compared, as shown in Figure 3. The model foundation is a 50.8 mm wide steel plate placed on the ground surface was experimentally examined by Badie [5]. Badie tested a strip foundation with a void that is 122.4 mm in diameter and located at 101.6 mm under the footing surface. The axis of the void is parallel and centered with the footing axis. The soil type is commercial kaolin. The soil properties: E_{soil} = 19.86 Mpa, v = 0.39, C = 158.6 kpa, φ = 8 degrees, dry unit weight =13.5 kN/m^3.

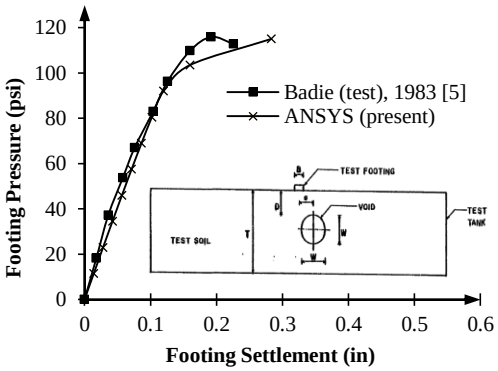

Figure 3: Comparison of ANSYS analysis results and model test developed by Badie [5]

The results showed a good agreement with those presented by Badie [5], which indicates that the ANSYS model is a good tool to predict the behavior of the surface structures resting on soil with voids. In the following part, a wide range of parameters are considered such as, (structure width and height, void diameter, and void vertical and horizontal distance from the center of the building raft) to investigate the performance of the reinforced concrete buildings above soil containing voids.

2.4 Parametric Study

A three-dimensional model of a reinforced concrete structure resting on soil with a uniform continuous circular void was analyzed using ANSYS. Three areas of RC structure (10*10 m^2), (20*20 m^2), and (30*30 m^2) were analyzed with two different heights, four floors with 12 m height and ten floors with 30 m height to study the effect of void location and its size in the soil beneath different sizes of structures. Figure 4 shows the six RC structures studied in this analysis. Tables 1 and 2 show the dimensions and reinforcement of all the examined structures.

Table 1: Dimensions and reinforcement of structures ST 1, ST 2, and ST3.

Structure	ST 1	ST 2	ST 3
Floor Area (m^2)	10*10	20*20	30*30
Height *H* (m)	12	12	12
No. of floors *n*	4	4	4
Raft Dim. *B***B* (m^2)	12.5x12.5	22.5x22.5	32.5x32.5
Raft thickness t_s (m)	0.6	0.6	0.6
Dim. of beams (m^2)	0.3x0.6	0.3x0.6	0.3x0.6
Dim. (m) and RFT of external columns	0.4x0.4 8φ 18mm	0.4x0.4 8φ 18mm	0.4x0.4 8φ 18mm
Dim. (m) and RFT of internal columns	0.4x0.4 8φ 18mm	0.4x0.4 8φ 18mm	0.4x0.4 8φ 18mm
RFT. of top beam	3φ 16mm	3φ 16mm	3φ 16mm
RFT. of bottom beam	3φ 16mm	3φ 16mm	3φ 16mm

Table 2: Dimensions and reinforcement of structures ST 4 ST 5, and ST6.

Structure	ST 4	ST 5	ST 6
Floor Area (m^2)	10*10	20*20	30*30
Height *H* (m)	30	30	30
No. of floors *n*	10	10	10
Raft Dim. *B***B* (m^2)	12.5x12.5	22.5x22.5	32.5x32.5
Raft thickness t_s (m)	1	1	1
Dim. of beams (m^2)	0.3x0.6	0.3x0.6	0.3x0.6
Dim. (m) and RFT of external columns	0.4x0.4 8φ 25mm	0.4x0.4 8φ 25mm	0.4x0.4 8φ 25mm
Dim. (m) and RFT of internal columns	0.5x0.7 12φ25mm	0.5x0.7 12φ25mm	0.5x0.7 12φ25mm
RFT. of top beam	3φ 16mm	3φ 16mm	3φ 16mm
RFT. of bottom beam	3φ 16mm	3φ 16mm	3φ 16mm

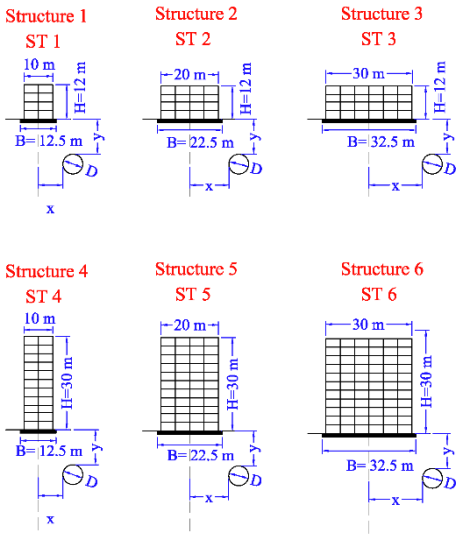

Figure 4: The geometry of examined structures and the key parameters studied.

The foundation performance above voids is affected by the void location and diameter. In each structure, sixty cases of different void diameters and locations were studied. Three void diameters of (*D*= 6.25, 12.5, and 25 m) were used in this parametric study, located at distances *x*= 0.5*B*, *B*, 2*B*, and 3*B* horizontally from the c.g of the footing, and one centered under the footing at depth *y*= 0.5*B*, *B*, 2*B*, and 3*B* vertically from the footing surface for each structure. Where, *B* refers to raft width, *x* and *y* refer to the void edge eccentricity and void depth from the ground surface, respectively. Figure 5 shows the all-void cases studied in this parametric study for each structure.

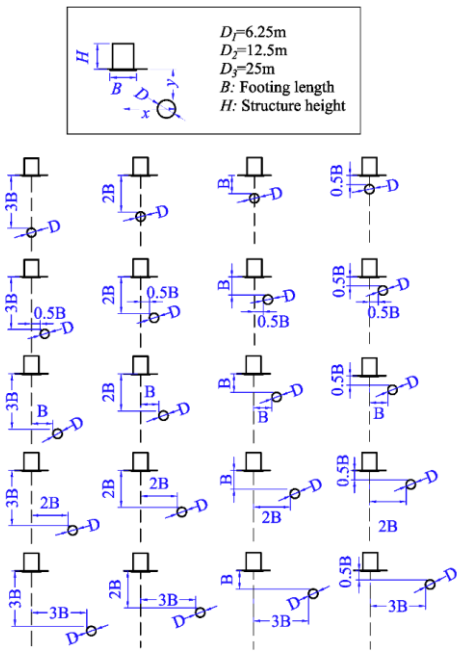

Figure 5: The problem geometry of all sixty cases studied for each structure

3 RESULTS AND DISCUSSION

Numerous factors affect the size of the void critical region, such as footing's shape, building size, soil properties, and void's size and location. Whenever the underground void is situated in the critical area, the placement of the void has a significant impact on the footing behavior [6]. From the results obtained from the current parametric study, the main factors which have effects on the critical regions under the structures will be discussed in the following parts.

3.1 The influence of void diameter and its location

Charts in Figures 6, 8, and 10 show the effect of void diameter and its location on the settlement ratio (s/s_o) that occurred beneath the center of the concrete raft for structures 1, 2, and 3. Where s refers to the settlement beneath the footing center and s_o presents the settlement under the footing center in the case of no underground void.

For structure 1, with centric void located at depth y equal to 0.5B=6.25m, the increase in settlement occurred beneath the center of the concrete raft due to void diameters D= 6.25, 12.5, and 25m are 17.8, 48.4, and 114.9 %, respectively. When the void is located symmetrically at depth y equal to 1B under the structure, the increase in settlement occurred beneath the center of the concrete raft due to void diameter D= 6.25, 12.5, and 25m are 7.4, 18.3, and 43.9 % respectively. When the void is located symmetrically at depth y equal to 2B under the structure, the increase in settlement occurred beneath the center of the concrete raft due to void diameter D= 6.25, 12.5, and 25m are 2.3, 4.6, and 10 %, respectively. Then at more depths, the effect of the void can be ignored.

For structure 2, with centric void located at depth y equal to 0.28B=6.25m, the increase in settlement occurred beneath the center of the concrete raft due to void diameters D= 6.25, 12.5, and 25m are 13.6, 37.9, and 101 %, respectively. At void depth y equals 0.5B, the increase in settlement occurred beneath the center of the concrete raft due to void diameter D= 6.25, 12.5, and 25m are 8.6, 23.9, and 60 %, respectively. When the void is located symmetrically at depth y equals 1B under the structure, the increase in settlement occurred beneath the center of the concrete raft due to void diameter D= 6.25, 12.5, and 25m are 4.4, 9.7, and 21.3 %, respectively. When the void is located symmetrically at depth y equal to 2B under the structure, the increase in settlement occurred beneath the center of the concrete raft due to void diameter D= 6.25, 12.5, and 25m are 0.9, 2.4, and 4.3 %, respectively.

For structure 3, with a centric void located at depth y equal to 0.19B=6.25m, the increase in settlement occurred beneath the center of the concrete raft due to void diameters D= 6.25, 12.5, and 25m are 9.3, 30.2, and 86.9 %, respectively. At void depth y equals 0.5B, the increase in settlement occurred beneath the center of the concrete raft due to void diameter D= 6.25, 12.5, and 25m are 5.2, 13.2, and 36.6 %, respectively. When the void is located symmetrically at depth y equal to 1B under the structure, the increase in settlement occurred beneath the center of the concrete raft due to void diameters D =6.25, 12.5, and 25m are 2.2, 4.4, and 12.7 %, respectively. Then at more depths, the effect of the void can be ignored.

From the results above, it was obtained that the influence of underground void decreases as the void depth ratio y/B and the void eccentricity ratio x/B increase. It was found that the critical void eccentricity and depth ratios (x_{cr}/B and y_{cr}/B) increase as the void diameter increases for the same structure, as shown in Figure 12. For structure 1, the critical void depth ratios y_{cr}/B were 2, 3, and 3.5, and the critical void eccentricity ratios x_{cr}/B were 1, 1.5, and 1.75 for void diameters 6.25, 12.5, and 25 m, respectively. The other six structures followed the same trend.

Figures 7, 9, and 11 show the differential settlement ratio or footing rotation ($\Delta s/B$) with void eccentricity ratio (x/B) for various void depth ratios (y/B) for structures 1, 2, and 3, the solid lines in the curves show the results obtained from the analyses and the dashed lines refer to the expected results only not calculated. The differential settlement ratio $\Delta s/B$ calculated as (s_1-s_2)/B. s_1 and s_2 are the settlements of the base edges due to the location of the eccentric void and B (the raft width) represents the distance between these edges. However, the void depth ratio y/B is more effective than the eccentric void ratio x/B in a variation of maximum

settlement under the structure footing, the eccentric void ratio *x/B* needs more attention because it influences stability and tilting of the building. The footing rotation increases with increasing the eccentric void ratio *x/y* from the footing center, and it reaches the maximum value when the void center is located exactly under each of the footing edges, then it decreases again when the void is located far away from the footing. At *x/B* approximately equal to 2, the footing rotation becomes zero. The differential settlement ratio or the footing rotation increases as the void depth ratio decreases and the void diameter increases.

3.2 The influence of structure width *B*

From the results for structures 1, 2, and 3 of the same height but various footing widths B, it was found that the critical void eccentricity and void depth ratios (x_{cr}/B) and (y_{cr}/B) decrease with increasing in footing width *B* for each specific void diameter *D*, as shown in figure 12.

For underground void diameter *D* equals to 6.25m located below the three structures, the critical void eccentricity ratios (x_{cr}/B) for structures 1, 2, and 3 are 1, 0.75, and 0.5, respectively, and the critical void depth ratios (y_{cr}/B) are 2, 1.5, and 1, respectively. For underground void diameter *D* equals to 12.5m located below the three structures, the critical void eccentricity ratios (x_{cr}/B) for structures 1, 2, and 3 are 1.5, 1, and 0.75, respectively, and the critical void depth ratios (y_{cr}/B) are 3, 2, and 1.5, respectively. Finally, for underground void diameter *D* equal to 25m located below the three structures, the critical void eccentricity ratios (x_{cr}/B) for structures 1, 2, and 3 are 1.75, 1.5, and 1 respectively, and the critical void depth ratios (y_{cr}/B) are 3.5, 3, and 2, respectively, as shown in Figure 13. It was observed that the critical void eccentricity and depth distances x_{cr} and y_{cr} are almost the same value for structures 2 and 3 for each specific diameter, but these values are more than the case of structure 1, as shown in the charts in Figure 14. It was found that in the same condition of the void, the effect of the void (settlement ratio (s/s_o)) decreases significantly as the structure width increases. It means that wide structures are preferable in the soil which contains voids.

The differential settlement ratio or the footing rotation is slightly affected by footing width. The values are close to each other for various footing widths *B* with the same height *H* under the same void conditions, as shown in Figure 18.

3.3 The influence of structure height *H*

The structure height has no effects on void critical locations, but there is a small decrease value in settlement ratios s/s_0 in the case of higher buildings compared to the lower buildings with the same width, as shown in Figures 15, 16, and 17. For a specific void diameter, the differential settlement ratio between the footing edge ($\Delta s/B$) (footing rotation) increases as the structure height increases, as shown in Figure 18.

Figure 19 shows the distribution of settlement that occurred beneath structure 3 for the most effective cases of void locations of void diameter equal to 25m compared to the case without underground voids. This figure shows the effect of void locations in the distribution of deformations under the structures.

3.4 Proposed Equation for the Critical Void Location

From the results of the values of the critical locations for the six structures with various widths and heights, two equations were developed to present the critical underground void location beneath the surface structures, as indicated in Figure 20. These equations are a useful tool in designing concrete structures with squared rafts resting above soil containing void, at least in the range of parameters that have been studied. The following equations Eqs. (1) and (2) estimate the critical void depth ratio (y_{cr}/B) and critical void eccentricity ratio (x_{cr}/B) according to the void diameter D and the squared footing width B:

$$y_{cr}/B = 0.08D + 2.2788\, e^{-0.002B^2} \quad (1)$$

$$x_{cr}/B = 0.04D + 1.1394\, e^{-0.002B^2} \quad (2)$$

Where; Diameter (*D*) is from 6.25 to 25 m, and squared footing width (*B*) is from 10 to 30 m.

Void depth *y* is more effective in increasing the maximum settlement beneath the structure center than the void eccentricity, in which critical void depth y_{cr} is always twice of critical void eccentricity x_{cr}. But it was shown that void eccentricity *x* has more effects on the stability of the structure as it causes differential settlement between the edges of the footings.

3.5 Settlements and Differential Settlement Limits

According to The Egyptian Code for Soil Mechanics and Foundation Implementation, the allowable maximum settlement for buildings resting on shallow foundations on clay soils ranges from 100 to 150 mm [32].

The maximum settlements under the footing center of ST1, ST2, ST3, ST4, ST5, and ST6 without a void equal 4.88, 12.37, 20.84, 11.2, 27.14, and 44.43 mm, respectively. All the investigated void cases under the structures led to an increase in the settlements under the footing. The recorded worst void case was the centric void at a void depth *y* equal to 6.25m with a void diameter *D* of 25m. This void case increased the settlement value under the center of the footings to 10.49, 24.9, 38.9, 25.3, 50.77, and 74.14 mm for ST1, ST2, ST3, ST4, ST5, and ST6, respectively. The settlement values are still below the code limits. Therefore, it is necessary to check the settlements under the footings before construction on soil containing

underground voids if the void is located within the critical void zone.

The allowable differential settlement ratio $(s_1-s_2)/B$ is 0.0067, according to The Egyptian Code for Soil Mechanics and Foundation Implementation [32]. The recorded worst void case that caused maximum differential settlements within the studied cases was the eccentric void of 25m in diameter with an eccentric void ratio x/B equal to 0.5 at a void depth y equal to 6.25m. This void case caused differential settlement ratios 0.0008, 0.00017, 0.00019, 0.00024, 0.00038, and 0.00043 mm for ST1, ST2, ST3, ST4, ST5, and ST6, respectively. The differential settlement ratios are still below the code limits. It is necessary to check the differential settlement ratio before construction on soil containing underground voids, especially for small buildings.

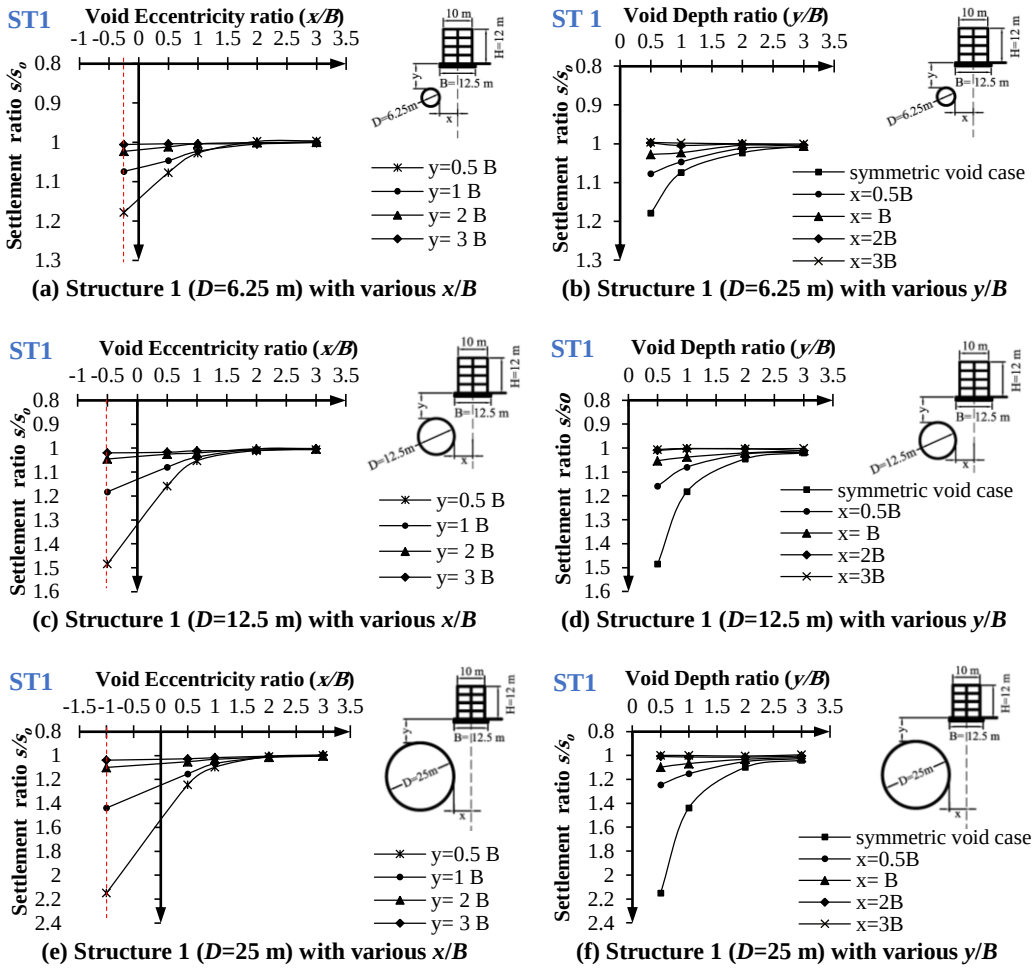

Figure 6: Variations of settlement ratio (s/s_0) at the footing center, with Void Eccentricity ratio (x/B) for various void depths ratio (y/B) for structure 1

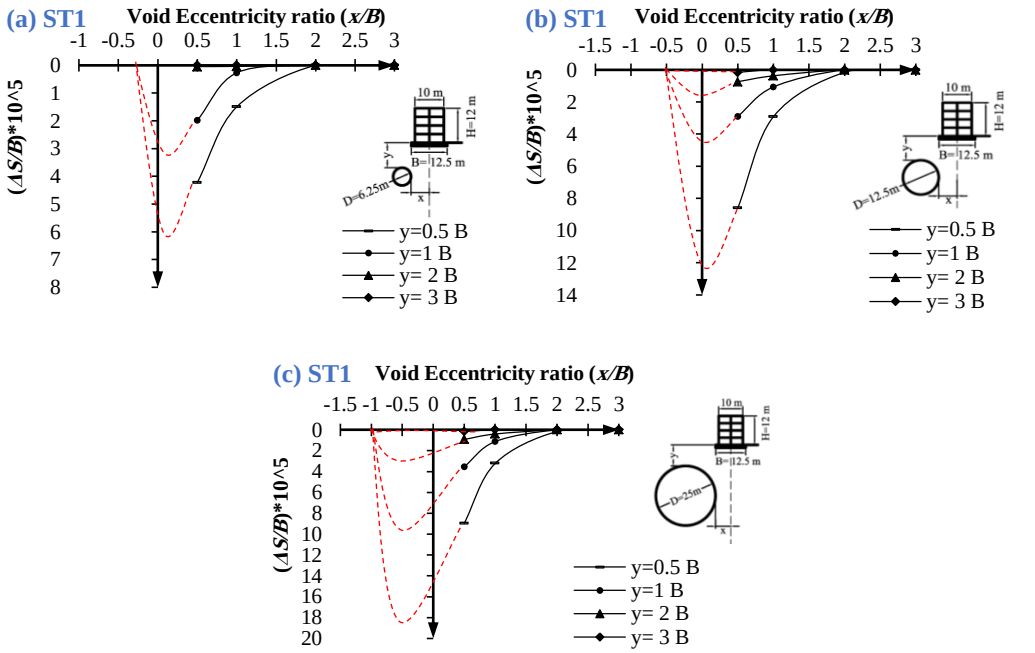

Figure 7: Differential settlement ratio ($\Delta s/B$) with void eccentricity ratio (x/B) for various void depths ratio (y/B) for ST 1; (a) D=6.25m, (b) D=12.5m and (c) D=25m

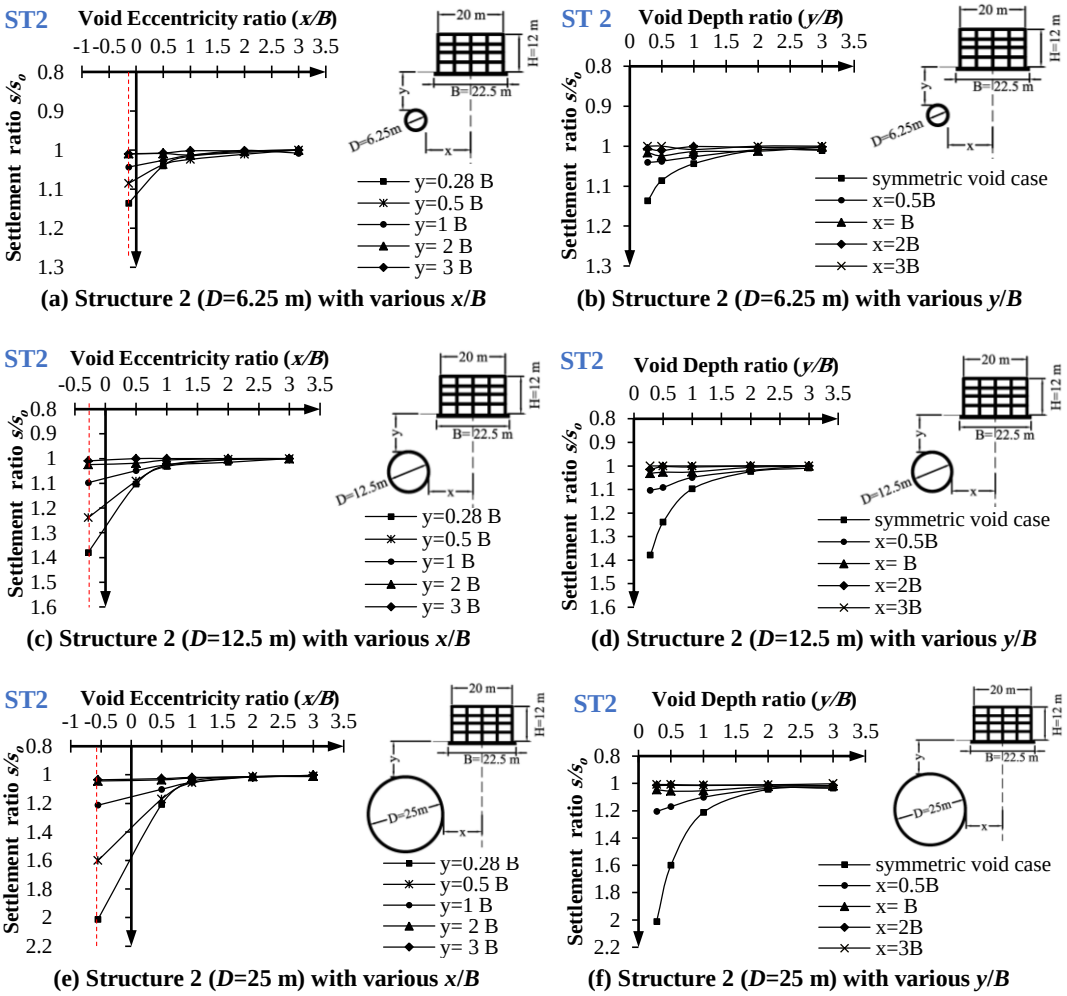

Figure 8: Variations of settlement ratio (s/s_0) at the footing center, with void eccentricity ratio (x/B) for various void depths ratio (y/B) for structure 2

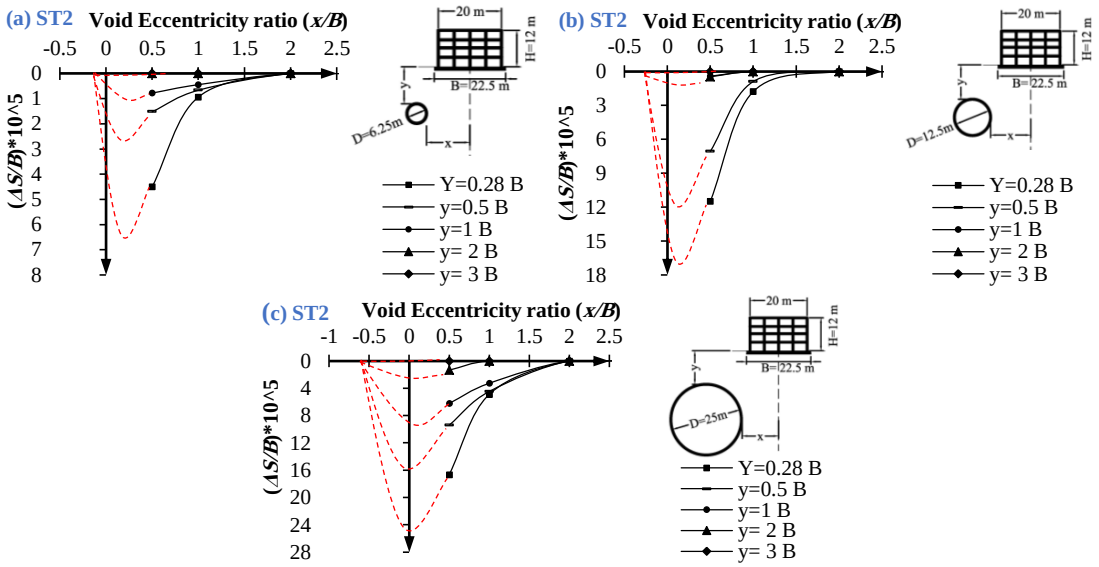

Figure 9: Differential settlement ratio ($\Delta s/B$) with void eccentricity ratio (x/B) for various void depths ratio (y/B) for ST 2;

(a) D=6.25m, (b) D=12.5m and (c) D=25m

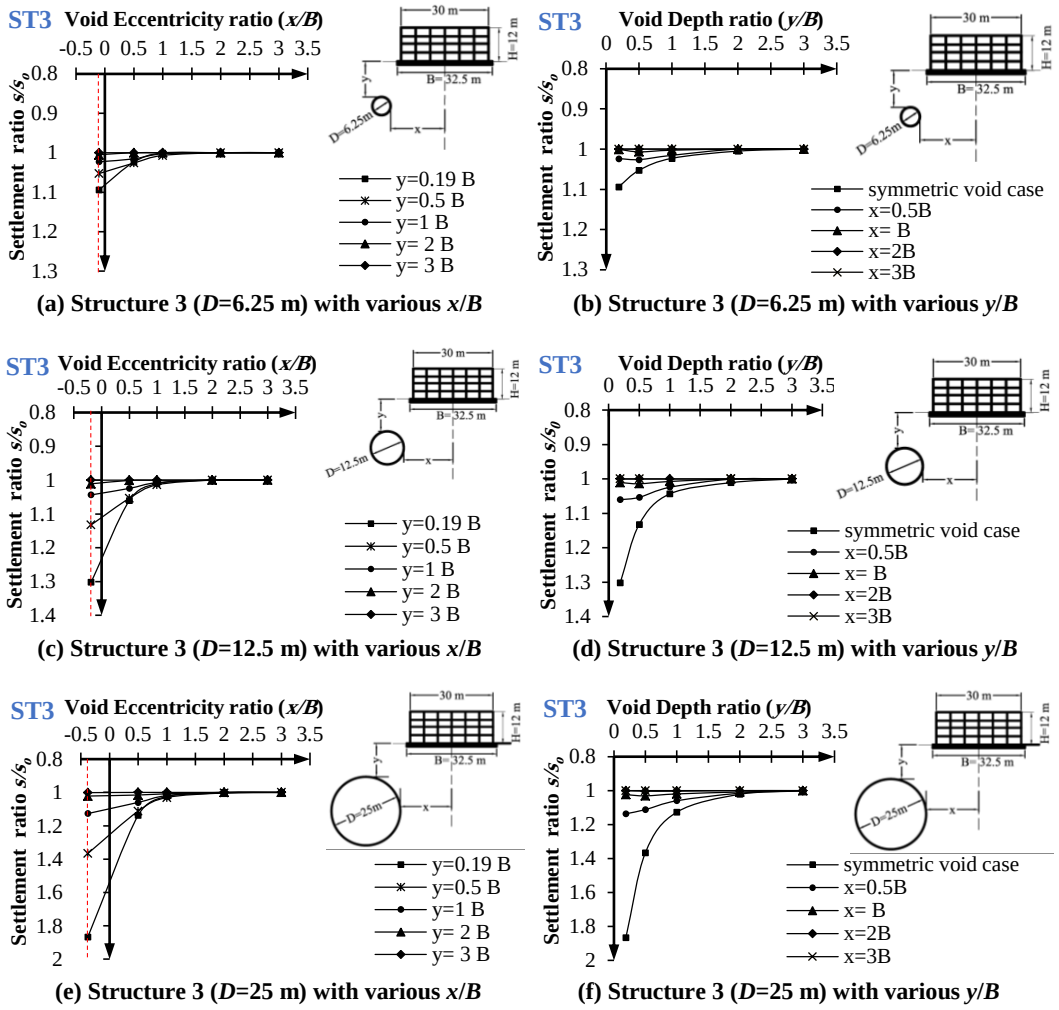

(a) Structure 3 (D=6.25 m) with various x/B (b) Structure 3 (D=6.25 m) with various y/B

(c) Structure 3 (D=12.5 m) with various x/B (d) Structure 3 (D=12.5 m) with various y/B

(e) Structure 3 (D=25 m) with various x/B (f) Structure 3 (D=25 m) with various y/B

Figure 10: Variations of settlement ratio (s/s_0) at the footing center, with void eccentricity ratio (x/B) for various void depths ratio (y/B) for structure 3

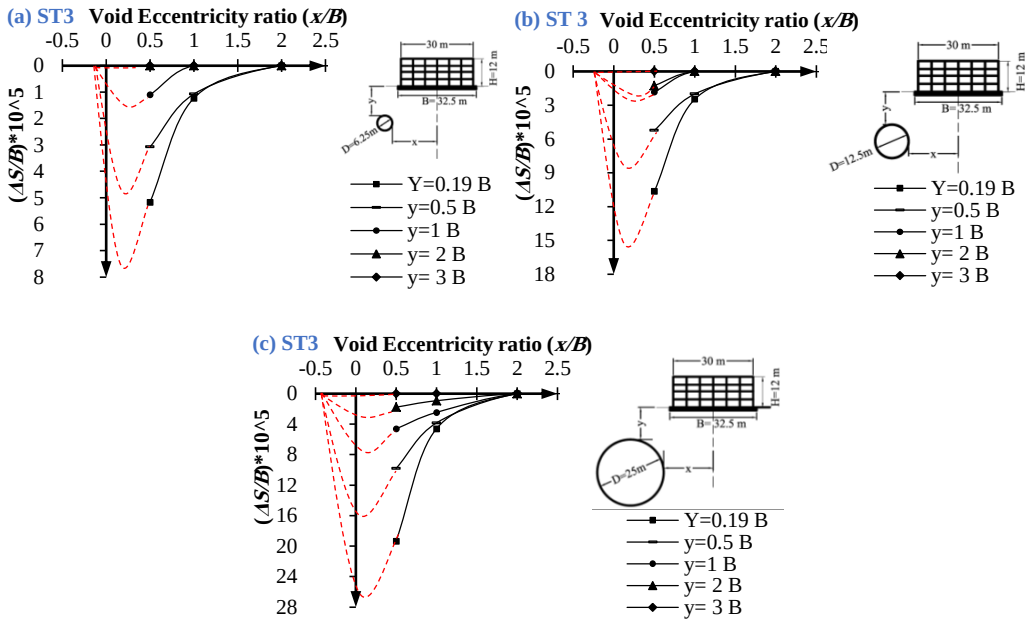

Figure 11: Differential settlement ratio ($\Delta s/B$) with void eccentricity ratio (x/B) for various void depths ratio (y/B) for ST 3; (a) D=6.25m, (b) D=12.5m and (c) D=25m

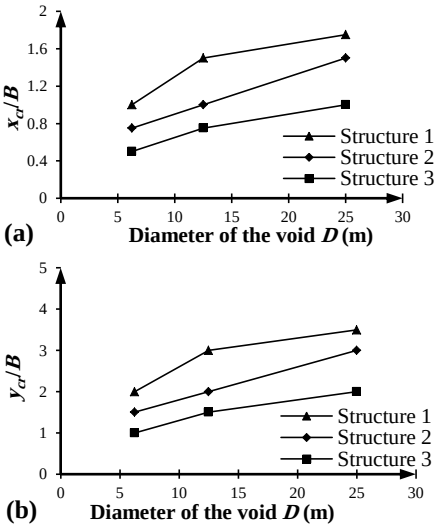

Figure 12: Comparison of critical void location ratios for various diameters for different sizes of structures; (a) x_{cr}/B, and (b) y_{cr}/B

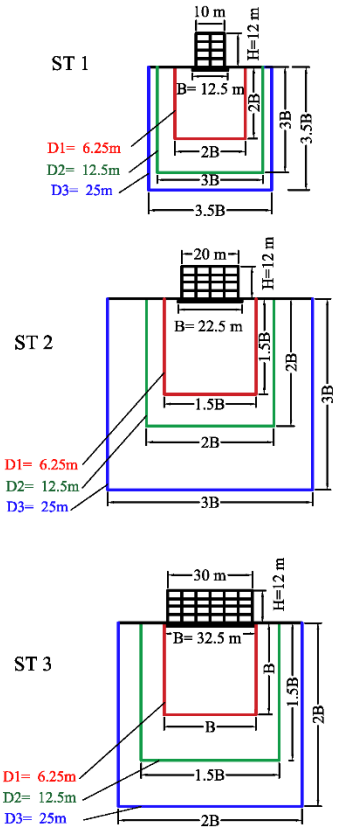

Figure 13: Critical void locations for various diameters for structures 1,2, and 3

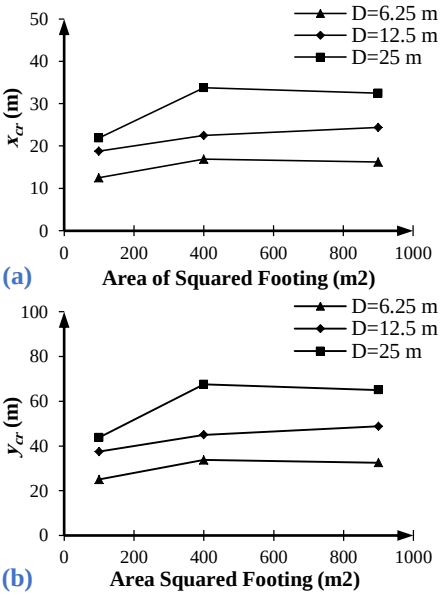

Figure 14: Comparison of critical void distances for various diameters for different sizes of structures; (a) critical void eccentricity distance x_{cr}, and (b) critical void depth distance y_{cr}

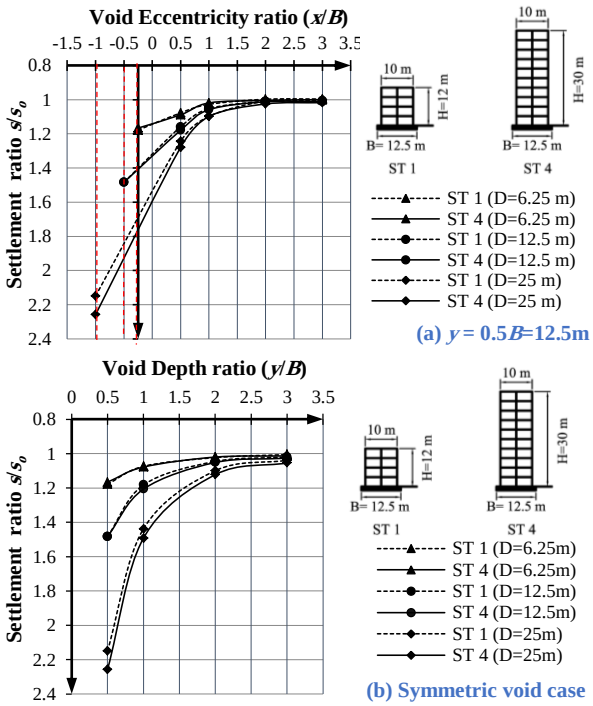

Figure 15: Comparison of settlement ratio (s/s_0) at the footing center; (a) with void eccentricity ratio (x/B) at void depth ratio (y/B) =0.5, and (b) with various depth ratios (y/B) for a symmetric void case for ST 1 and ST 4.

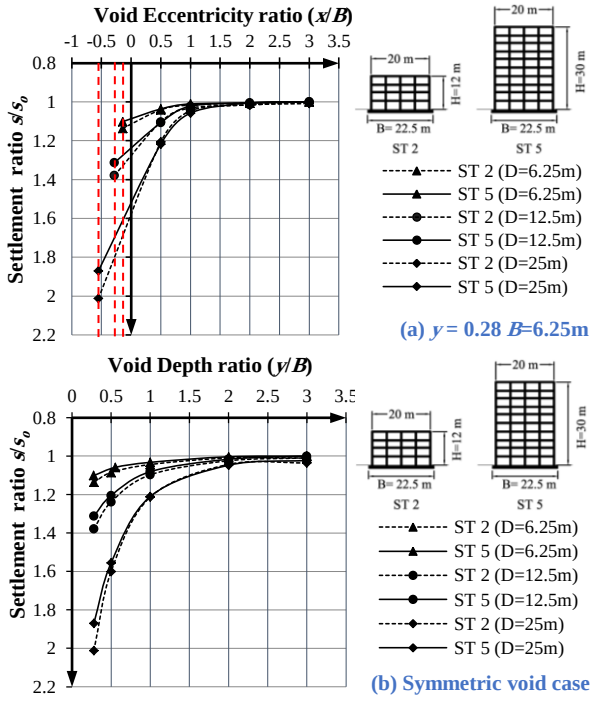

Figure 16: Comparison of settlement ratio (s/s_0) at the footing center; (a) with void eccentricity ratio (x/B) at void depth ratio (y/B) =0.28, and (b) with various depth ratios (y/B) for a symmetric void case for ST 2 and ST 5.

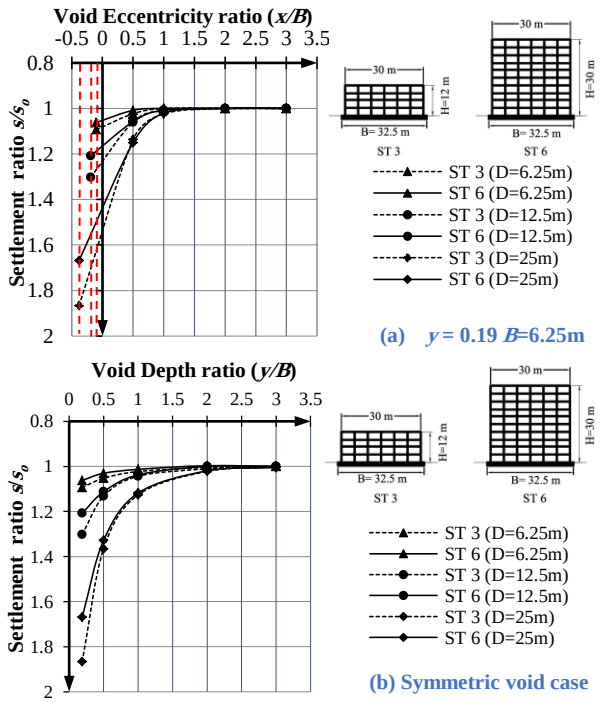

Figure 17: Comparison of settlement ratio (s/s_0) at the footing center; (a) with void eccentricity ratio (x/B) at void depth ratio (y/B) =0.19, and (b) with various depth ratios (y/B) for a symmetric void case for ST 3 and ST 6.

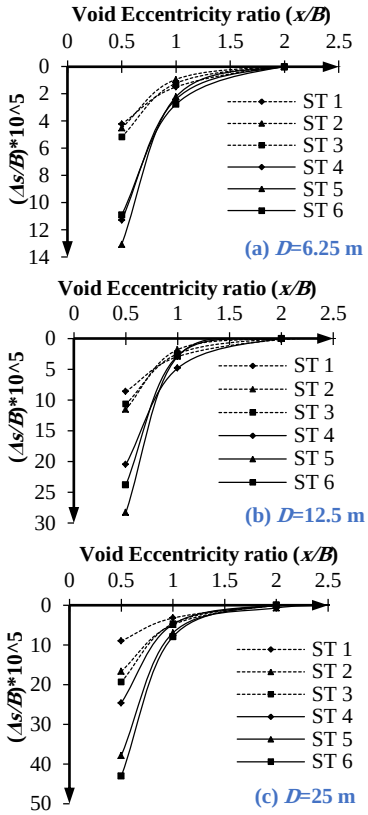

Figure 18: Comparison of differential settlement between footing edges ratio ($\Delta s/B$) for various diameters for different sizes of structures; (a) D=6.25m, (b) D=12.5 m, and (c) D=25m

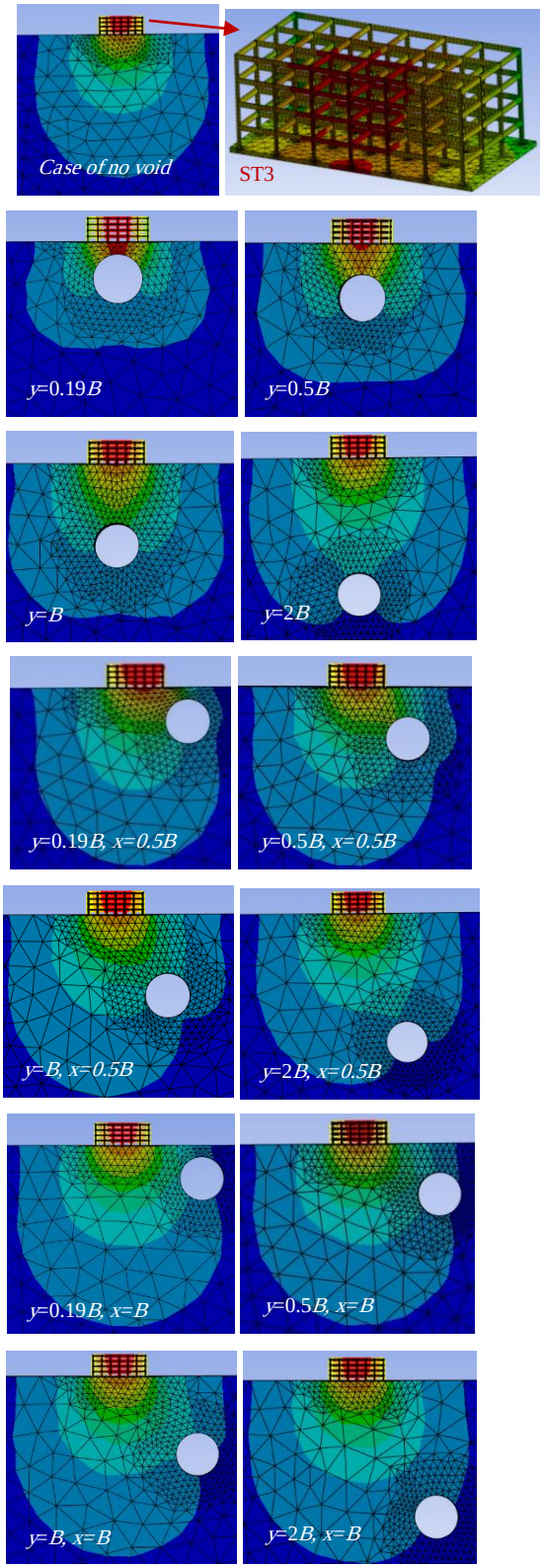

Figure 19: Variations of vertical deformation for (ST 3) rested on soil with 25m of void diameter for most effective void locations *x* and *y*

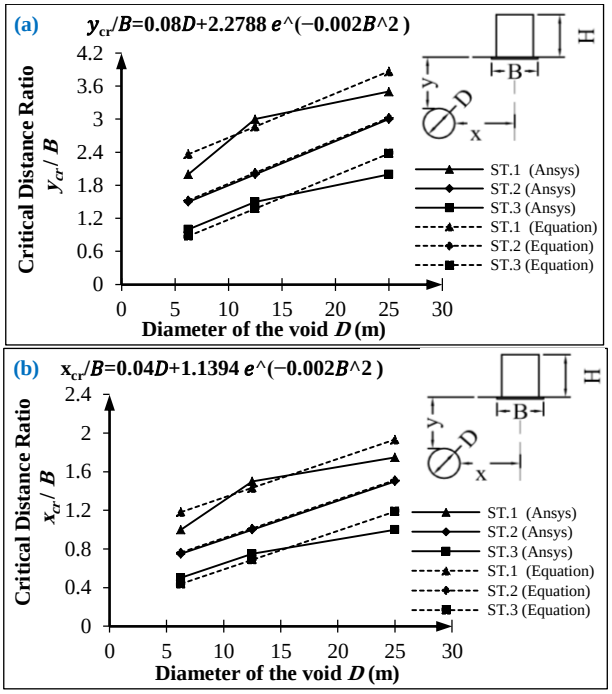

Figure 20: Critical void locations x_{cr} and y_{cr} equations; (a) Estimation of y_{cr}, and (b) Estimation of x_{cr}

4 CONCLUSIONS

In this study, three-dimensional models of six concrete buildings with squared raft footings were analyzed using ANSYS computer program. It was simulated that the concrete structures are founded on clay soil containing continuous circular voids. The parameters considered in this analysis are structure height *H*, squared footing width *B*, void diameter *D*, and void locations (eccentricity and depth from the ground surface). The settlement ratio under footing center (s/s_0) and differential settlements (footing rotation) occurred due to void eccentricity were estimated for each case. The effects of the parameters mentioned above were examined and concluded as follows:

- The footing squared area (or squared footing width *B*) has great effects on the prediction of critical void location that the critical void location ratios (x_{cr}/B and y_{cr}/B) decrease as the footing width *B* increases for the same void diameter.
- The structure height doesn't have any effect on the critical void location values for structures having the same footing width *B*.
- For a specific void diameter, the differential settlement ratio between the footing edge ($\Delta s/B$) (footing rotation) increases as the structure height increases and is still almost constant for structures having the same height with various widths.
- The critical void eccentricity and depth ratios increase as the void diameter increases.

- Two equations were introduced for estimating the critical void location under the concrete structures according to the footing width and void diameter. It is shown that these equations introduce simple tools to predict the critical void location within the variety of parameters that have been studied in this study.

Author contribution:

Aya G. Abdel-Nasser: Methodology, Validation, Formal analysis, Data curation, and writing original draft, Investigation. ***Emad Y. Abdel-Galil:*** Methodology, Data curation, Writing-review and editing, Visualization, and Supervision. ***Ezzaat A. Sallam:*** Validation, Formal analysis, writing-review and editing, Visualization, Investigation, and Supervision. All authors have read and agreed to the published version of the manuscript.

Competing interests: The authors declare there are no competing interests.

Funding : The authors declare no specific funding for this work.

5 REFERENCES

[1] J. K. Lee, S. Jeong, and J. Ko, "Undrained stability of surface strip footings above voids," *Computers and* Geotechnics, vol. 62, pp. 128-135, 2014. https://doi.org/10.1016/j.compgeo.2014.07.009.

[2] A. Asakereh, M. Ghazavi, and S. M. Tafreshi, "Cyclic response of footing on geogrid-reinforced sand with void," *Soils and foundations*, vol. 53, no. 3, pp. 363-374, 2013. https://doi.org/10.1016/j.sandf.2013.02.008

[3] R. L. Baus, *The stability of shallow continuous footings located above voids*. The Pennsylvania State University, 1980.

[4] R. Baus and M. Wang, "Bearing capacity of strip footing above void," *Journal of Geotechnical Engineering*, vol. 109, no. 1, pp. 1-14, 1983. https://doi.org/10.1061/(ASCE)0733-9410(1983)109:1(1).

[5] A. Badie, *Stability of spread footing supported by clay soil with an underground void*. The Pennsylvania State University, 1983.

[6] A. Badie and M. Wang, "Stability of spread footing above void in clay," *Journal of Geotechnical Engineering*, vol. 110, no. 11, pp. 1591-1605, 1984. https://doi.org/10.1016/0148-9062(85)93766-0.

[7] M. Wang and A. Badie, "Effect of underground void on foundation stability," *Journal of Geotechnical Engineering*, vol. 111, no. 8, pp. 1008-1019, 1985. https://doi.org/10.1061/(asce)0733-9410(1985)111:8(1008).

[8] M. Wang and C. Hsieh, "Collapse load of strip footing above circular void," *Journal of geotechnical engineering*, vol. 113, no. 5, pp. 511-515, 1987. https://doi.org/10.1061/(asce)0733-9410(1987)113:5(511).

[9] B. W. Jaroudi, "Collapse Pressure of Strip Footing Underlain by Ecentric Continuous Circular Void," Pennsylvania State University, 1987.

[10] A. Badie and M. Wang, "Stability of Underground Cavity subjected to Surface Loads," in *International Symposium on Unique Underground Structures, Denver, Colorado*, 1990.

[11] C. Hsieh and M. Wang, "Bearing capacity determination method for strip surface footings underlain by voids," *Transportation Research Record*, no. 1336, 1992.

[12] M. Kiyosumi, O. Kusakabe, M. Ohuchi, and F. Le Peng, "Yielding pressure of spread footing above multiple voids," *Journal of Geotechnical and Geoenvironmental Engineering*, vol. 133, no. 12, pp. 1522-1531, 2007. https://doi.org/10.1061/(asce)1090-0241(2007)133:12(1522).

[13] M. Kiyosumi, O. Kusakabe, and M. Ohuchi, "Model tests and analyses of bearing capacity of strip footing on stiff ground with voids," *Journal of geotechnical and geoenvironmental engineering*, vol. 137, no. 4, pp. 363-375, 2011. https://doi.org/10.1061/(ASCE)GT.1943-5606.0000440.

[14] J. K. Lee and J. Kim, "Stability charts for sustainable infrastructure: Collapse loads of footings on sandy soil with voids," *Sustainability*, vol. 11, no. 14, p. 3966, 2019. https://doi.org/10.3390/su11143966.

[15] A. A. Lavasan, A. Talsaz, M. Ghazavi, and T. Schanz, "Behavior of shallow strip footing on twin voids," *Geotechnical and Geological Engineering*, vol. 34, pp. 1791-1805, 2016. https://doi.org/10.1007/s10706-016-9989-6.

[16] L. Zhao, S. Huang, R. Zhang, and S. Zuo, "Stability analysis of irregular cavities using upper bound finite element limit analysis method," *Computers and Geotechnics*, vol. 103, pp. 1-12, 2018. https://doi.org/10.1016/j.compgeo.2018.06.018.

[17] C. Hsieh, *Footing behavior and stability analysis method for strip surface footing above continuous circular void*. The Pennsylvania State University, 1991.

[18] G. Azam, C. Hsieh, and M. Wang, "Performance of strip footing on stratified soil deposit with void," *Journal of geotechnical engineering*, vol. 117, no. 5, pp. 753-772, 1991. https://doi.org/10.1016/0148-9062(91)91512-p.

[19] B. Das and K. Khing, "Foundation on layered soil with geogrid reinforcement—effect of a void," *Geotextiles and Geomembranes*, vol. 13, no. 8, pp. 545-553, 1994. https://doi.org/10.1016/0266-1144(94)90018-3.

[20] S. Sireesh, T. Sitharam, and S. K. Dash, "Bearing capacity of circular footing on geocell–sand mattress overlying clay bed with void," *Geotextiles and Geomembranes*, vol. 27, no. 2, pp. 89-98, 2009. https://doi.org/10.1016/j.geotexmem.2008.09.005.

[21] S. Moghaddas Tafreshi, O. Khalaj, and M. Halvaee, "Experimental study of a shallow strip footing on geogrid-reinforced sand bed above a void," *Geosynthetics International*, vol. 18, no. 4, pp. 178-195, 2011. https://doi.org/10.1680/gein.2011.18.4.178.

[22] M. M. A. Hussein, "Stability of strip footing on sand bed with circular void," *JES. Journal of Engineering*

Sciences, vol. 42, no. 1, pp. 1-17, 2014. https://doi.org/10.21608/jesaun.2014.111011.

[23] J. Jayamohan, T. Shajahan, and A. Sasikumar, "Effect of underground void on the internal stress distribution in soil," in *Ground Improvement Techniques and Geosynthetics: IGC 2016 Volume 2*, 2019: Springer, pp. 45-56, doi: 10.1007/978-981-13-0559-7_6.

[24] S. Anaswara and R. Shivashankar, "Study on behaviour of two adjacent strip footings on granular bed overlying clay with a void," *Transportation Infrastructure Geotechnology*, vol. 7, pp. 461-477, 2020. https://doi.org/10.1007/s40515-020-00122-x.

[25] B. Mazouz, T. Mansouri, M. Baazouzi, and K. Abbeche, "Assessing the Effect of Underground Void on Strip Footing Sitting on a Reinforced Sand Slope with Numerical Modeling," *Engineering, Technology & Applied Science Research*, vol. 12, no. 4, pp. 9005-9011, 2022. https://doi.org/10.48084/etasr.5131.

[26] Y. Xiao, M. Zhao, and H. Zhao, "Undrained stability of strip footing above voids in two-layered clays by finite element limit analysis," *Computers and Geotechnics*, vol. 97, pp. 124-133, 2018. https://doi.org/10.1016/j.compgeo.2018.01.005.

[27] H. Zhou, G. Zheng, X. He, X. Xu, T. Zhang, and X. Yang, "Bearing capacity of strip footings on c–φ soils with square voids," *Acta Geotechnica*, vol. 13, pp. 747-755, 2018. https://doi.org/10.1007/s11440-018-0630-0.

[28] M. Wang, C. Yoo, and C. Hsieh, "Effect of void on footing behavior under eccentric and inclined loads," in *Foundation Engineering: Current Principles and Practices*, 1989: ASCE, pp. 1226-1239.

[29] J. K. Lee, S. Jeong, and J. Ko, "Effect of load inclination on the undrained bearing capacity of surface spread footings above voids," *Computers and Geotechnics*, vol. 66, pp. 245-252, 2015. https://doi.org/10.1016/j.compgeo.2015.02.003.

[30] T. Mansouri, R. Boufarh, and D. Saadi, "Effects of underground circular void on strip footing laid on the edge of a cohesionless slope under eccentric loads," *Soils and Rocks*, vol. 44, 2021. https://doi.org/10.28927/SR.2021.055920.

[31] M. Z. Gaoqiao Wu, H. Zhao, and Y. Xiao, "Effect of Eccentric Load on the Undrained Bearing Capacity of Strip Footings above Voids," *International Journal of Geomechanics*, vol. 20, 2020. https://doi.org/10.1061/(ASCE)GM.1943-5622.0001710.

[32] ECP202, " The Egyptian Code for Soil Mechanics and Foundation Implementation (Part 3: Shallow Foundations)," *National Housing and Building Research Center: Cairo, Egypt.*, 2007.